Published in final edited form as:
Oncogene. 2012 November 29; 31(48): 4987–4995. doi:10.1038/onc.2011.653.

Sequential genetic change at the TP53 and chemokine receptor CXCR4 locus during transformation of human ovarian surface epithelium

Kyra M Archibald, PhD[1], **Hagen Kulbe, PhD**[1], **Joseph Kwong, PhD**[2], **Probir Chakravarty, BSc**[3], **Jill Temple, MSc**[4], **Tracy Chaplin, BSc**[5], **Magdalena B Flak, PhD**[6], **Iain A McNeish, PhD**[6], **Suha Deen, MD**[7], **James D Brenton, PhD**[4], **Bryan D Young, PhD**[5], and **Frances Balkwill, PhD**[1]

[1]Centre for Cancer and Inflammation, Barts Cancer Institute, Queen Mary University of London, London, UK

[2]Department of Obstetrics and Gynaecology, The Chinese University of Hong Kong, Hong Kong

[3]Bioinformatics and Biostatistics Service, 44 Lincoln's Inn Fields, London, UK

[4]Functional Genomics of Ovarian Cancer Laboratory, Cancer Research UK, Cambridge Research Institute, Li Ka Shing Centre, Cambridge, UK

[5]Centre for Haemato-Oncology, Barts Cancer Institute, Queen Mary University of London, London, UK

[6]Centre for Molecular Oncology, Barts Cancer Institute, Queen Mary University of London, London, UK

[7]Department of Histopathology, University Hospitals Nottingham, Nottingham, UK

Abstract

Early genetic events in the development of high-grade serous ovarian cancer, HGSOC, may define the molecular basis of the profound structural and numerical instability of chromosomes in this disease. To discover candidate genetic changes we sequentially passaged cells from a karyotypically normal hTERT immortalised human ovarian surface epithelial line (IOSE25) resulting in the spontaneous formation of colonies in soft agar. Cell lines (TOSE 1 and 4) established from these colonies had an abnormal karyotype and altered morphology but were not tumorigenic in immunodeficient mice.

TOSE cells showed loss of heterozygosity at *TP53*, increased nuclear p53 immunoreactivity and altered expression profile of p53 target genes. The parental IOSE25 cells contained a missense, heterozygous R175H mutation in *TP53* whereas TOSE cells had loss of heterozygosity at the *TP53* locus with a new R273H mutation at the previous wild-type *TP53* allele.

Cytogenetic and array CGH analysis of TOSE cells also revealed a focal genomic amplification of CXCR4, a chemokine receptor commonly expressed by HGSOC cells. TOSE cells had increased functional CXCR4 protein and its abrogation reduced epidermal growth factor receptor, EGFR, expression, as well as colony size and number. The CXCR4 ligand, CXCL12, was epigenetically silenced in TOSE cells and its forced expression increased TOSE colony size. TOSE cells had other cytogenetic changes typical of those seen in HGSOC ovarian cancer cell lines and biopsies.

Corresponding author: Frances Balkwill, f.balkwill@qmul.ac.uk. Telephone: (0)20 7882 3587 Fax: (0)20 7882 3885.

Conflict of interest The authors declare no conflict of interest.

Supplementary information is available at Oncogene's website.

Europe PMC Funders Author Manuscripts

In addition, enrichment of CXCR4 pathway in expression profiles from HGSOC correlated with enrichment of a mutated TP53 gene expression signature and of EGFR pathway genes.

Our data suggest that mutations in *TP53* and amplification of the *CXCR4* gene locus may be early events in the development of HGSOC, and associated with chromosomal instability.

Keywords

CXCR4; CXCL12; malignant transformation; high-grade serous ovarian cancer; p53

Introduction

During the past five years there have been major advances in our understanding of the cellular and molecular biology of the human malignancies collectively referred to as ovarian cancer. Pathological and genomic findings indicate that some ovarian cancers are derived from non-ovarian tissues and that the different histotypes share few molecular similarities (1). The major clinical feature that links 'ovarian' malignancies is frequent loco-regional dissemination to the ovary and related pelvic organs.

High-grade serous ovarian cancer, HGSOC, is the commonest and most lethal form, spreading throughout the peritoneum from its earliest stages. Although classically thought to arise from the ovarian surface epithelium or inclusion cysts (2) there is also strong evidence that HGSOC may arise from the adjacent fallopian tube epithelium (3-5). Mutations in the tumour suppressor *TP53* (6, 7), *BRCA* pathway disruption (8) and homologous recombination repair deficiency are the central genetic characteristics (1) and are associated with major structural and numerical chromosomal abnormalities (7). Although mutation of *TP53* is required for HGSOC, both clinical and *in vitro* studies suggest that it is not sufficient for transformation (9, 10).

Mouse models of HGSOC are complicated by significant differences in mouse anatomy and hormonal regulation. In order to accurately recapitulate this malignancy it is important that human cells are used. Karst *et al* (10) established immortalised human fallopian tube secretory epithelial cells with hTERT and either SV40 large and small T antigens or sh-p53. Such cells could be fully transformed by oncogenic Ras or c-myc so that they formed peritoneal malignancies in immunosuppressed mice. Similar, very recent studies confirmed these observations with multiple molecular alterations of primary human fallopian tube cells leading to immortalisation, senescence or full transformation (9). The finding of markers of genomic stress appears to be a unifying feature in these systems and also from studies of early invasions lesions in the fallopian tube (1, 11). Several years ago we also used hTERT to immortalise ovarian surface epithelial cells, IOSE, obtained from surface brushing of the ovary during surgery for benign conditions (12). More recently we monitored these IOSE cell lines for evidence of malignant transformation. Karyotypically normal immortalised cells from one of the donors spontaneously acquired the ability to grow in soft agar. These cells, that we have named TOSE, exhibited karyotypic abnormalities that are found in HGSOC tumours and cell lines, had altered p53 function through complex mutation events and amplification of the *CXCR4* gene locus at chromosome 2q21.3. This gene amplification was reflected in *de novo* expression of CXCR4 mRNA and functional CXCR4 protein.

As loss of p53 function is a central characteristic of HGSOC, and CXCR4 is commonly found on HGSOC cells (13, 14) where it is an important component of an autocrine tumor-promoting network (15), we suggest that TOSE cells may represent precursor cells of HGSOC and that CXCR4 expression may play a role in the earliest stages of this disease.

Europe PMC Funders Author Manuscripts

Results

Spontaneous 'transformation' of ovarian surface epithelial cells

We previously established hTERT immortalised human ovarian surface epithelial cell lines, IOSE, from three individuals. All lines had a 46,XX karyotype with functional p53 and Rb pathways (12). After repeated passage, one cell line, IOSE25, acquired the ability to form colonies in soft agar (Figure 1A). Cell populations were isolated from these colonies and named TOSE (transformed ovarian surface epithelium). Microsatellite analysis confirmed that TOSE clones were derived from IOSE25 (Supplementary table S1). Two clones, TOSE1 and 4 were further characterised. The morphology of TOSE1 and 4 cells was significantly altered, with an average circularity of 0.86±0.015 and 0.89±0.006 respectively, compared with 0.70±0.025 for IOSE25 (p=0.006 and 0.002). TOSE cells also showed increased nuclear staining for p53 (Figure 1B) and loss of heterozygosity (LOH) at the *TP53* gene locus (Figure 1C). p53 immunoreactivity generally correlates with increased p53 expression or altered stability, typically from missense mutations in the DNA binding domain (16). The transformed TOSE1 cells had increased expression of p53 target genes as compared to IOSE25 with significant up-regulation of 131 probes and down-regulation in 93 probes (Figure 1D and Supplementary table S2). Sanger sequencing of exons 2–11 of *TP53* showed that IOSE25 contained a heterozygous g.12512G>A mutation indicating a missense R175H amino acid substitution. TOSE1 and TOSE4 had identical *TP53* sequences with a g. 13798G>A mutation (R273H amino acid substitution) and g.12512G (wild-type codon 175). This is consistent with loss of heterozygosity at the *TP53* locus with a new R273H mutation in the previously normal allele (Supplementary Table S3). These data suggested that several populations of cells might have been originally present within the cultures and that selection for the R273H mutation occurred during enrichment of the transformed phenotype. To accurately quantitate the proportion of different *TP53* alleles during transformation we used digital PCR to determine the relative percentage of each mutated allele across a range of passages of IOSE25 cells and the donor normal NOSE25 cells from which the hTERT immortalised IOSE25 cells were derived (Figure 1E). None of the NOSE25 cells had the R273H mutation of *TP53*, but a very small population of cells exhibited a R175H mutation. Between passages 14 to 18 the IOSE25 cells still exhibited the R175H mutated allele but by passage 21 the TOSE cells displayed 100% prevalence of the R273H mutation.

As missense mutations in *TP53* may represent an early driver in HGSOC, we speculated that TOSE cells may reflect precursors of HGSOC cells. *TP53* mutation is infrequent in other types of 'ovarian' cancer (1). To further exclude the possibility that TOSE cells resembled low-grade serous ovarian cancer, we sequenced *KRAS* (exon 2), *BRAF* (exon 15), *CTNNB1* (exon 3) and *PIK3CA* (exon 10 and 21). No mutations were detected.

Cytogenetic abnormalities in TOSE cells

As genetic instability is a key characteristic of HGSOC we assessed the karyotype of TOSE 1 and 4 cells and found multiple abnormalities (46-77, XX, +X, +X, +X, add(1) (p21), +add(1), (q21), +der(?)t(1;?) (q25;?), +add(3) (q21), +6, add(6) (q2), +7, +7, +10, +10, +10, +10, ?der(11)t(11;13) (p11;q?13), +?der(11)t(11;13), +14, +14, +16, +16, +19, +20, +20, +21, +21, +2-8 mar, inc(cp5)).

Cytogenetic changes in TOSE cells and ovarian cancer samples

We next compared cytogenetic abnormalities in TOSE cells with published data for ovarian cancer cell lines and biopsies. Gains in 3q, 12p, 20q and losses in 8p and 17p are common to TOSE cells and high-grade serous ovarian cancers (17-21) (Supplementary Tables S4 and 5).

TOSE cells have a functional amplification of CXCR4

As copy number alterations have been shown to be drivers of HGSOC we carried out detailed copy number analysis using Affymetrix SNP6.0 arrays of the TOSE1 and TOSE4 cell lines, and a discrete copy number gain covering the *CXCR4* gene locus 2q 136,588,303-137,111,749 was found (Figure 2A). This amplicon contained two genes: *CXCR4* and *DARS*. *DARS* has no known role in ovarian cancer but CXCR4 is the only chemokine receptor commonly expressed on malignant ovarian epithelial cells in human cancer biopsies and cell lines (13, 22) and is implicated in ovarian cancer growth and spread (14, 15). *CXCR4* copy number gain was confirmed by fluorescent *in situ* hybridisation (Figure 2B: metaphase spread of TOSE1), and images quantified (Figure 2C). The chromosome 2 centromere was also duplicated in TOSE cells. As karyotyping did not detect extra copies of chromosome 2, we suggest that two extra truncated chromosome 2 are present in TOSE cells, one of which contains the extra *CXCR4*. *CXCR4* gene locus amplification was associated with increased CXCR4 mRNA levels in TOSE cells (Figure 2D) (see inset for CXCR4 protein western blot); this was localised at the cell surface as detected by flow cytometry (Figure 2E) and immunofluorescence (data not shown)

We tested the function of CXCR4 on TOSE cells using cell migration assays. IOSE cells did not migrate towards the sole ligand for CXCR4, CXCL12, but both TOSE lines gained this ability. Figure 3A shows a typical bell-shaped dose response curve for TOSE4 cells. This migration was CXCR4/CXCL12-specific as pre-incubation of the cells with two different CXCR4 antagonists, AMD3100 and CTCE9908, inhibited cell migration. TOSE cells did not migrate to another chemokine, CCL2 that binds to a different chemokine receptor, and neither IOSE nor TOSE cells expressed CXCR7, an alternative receptor for CXCL12 (23) (data not shown).

CXCR4 expression was stably silenced using shRNA (Figure 3B, C); this abrogated migration to CXCL12 (Figure 3D). In soft agar, shCXCR4 TOSE cell colony diameter was 50% of colony size from parental cells or scrambled shRNA controls (Figure 3E). There was also small but significant reduction in the number of colonies. Similar results were seen with shRNA in TOSE4 cells (data not shown). Hence we conclude that CXCR4 enhances growth in soft agar.

EGFR expression in TOSE cells

When compared with IOSE25 cells, TOSE1 cells also showed an increase in EGFR mRNA and protein. Stable knockdown of CXCR4 resulted in reduced EGFR mRNA (Figure 4A) and protein (Figure 4B), suggesting that CXCR4 is upstream of EGFR expression. Expression array analysis identified an enriched EGFR pathway in up-regulated genes in TOSE cells when compared with IOSE25 cells ($p=0.05$).

TOSE cells do not grow in immunocompromised mice

IOSE25, TOSE 1 and 4 cells were injected intraperitoneally, into the ovary, or subcutaneously into immunodeficient mice but no tumors were detected after eight to twelve weeks observation. A positive control, the HGSOC cell line IGROV-1, grew to form extensive tumours within four to six weeks in littermates. We also explored the counter-hypothesis that CXCR4 expression may keep the cells in a state of “low grade transformation” by injecting shCXCR4 TOSE1 cells or scrambled shRNA controls intraperitoneally or into the ovary of nude mice. IGROV-1 cells were again used as a positive control. Knockdown of CXCR4 did not render the TOSE1 cells tumorigenic after 10 weeks of observation.

TOSE cells are hypermethylated at the CXCL12 promoter

We previously reported that CXCR4-expressing malignant ovarian epithelial cells from advanced ovarian cancer also express the CXCR4 ligand CXCL12 *in vitro* and *in vivo* (13, 22, 24, 25). However, TOSE cells expressed very low levels of CXCL12 mRNA and protein when compared with IOSE25 cells (Figure 5A), or the ovarian cancer cell lines TOV21G and IGROV1 (15, 25). Epigenetic silencing of CXCL12 is found in colon and mammary carcinoma cells and is associated with metastasis to organs with high CXCL12 levels (26, 27).

We found that TOSE1 and TOSE4 cells were hypermethylated at the CXCL12 promoter (Figure 5B). Treatment of cells with the demethylating agent 5-azacytidine plus the HDAC inhibitor trichostatin A restored CXCL12 mRNA to a level of expression similar to the IOSE25 cells (Figure 5C).

Overexpression of CXCL12 in TOSE cells demonstrated no effect on the number of colonies formed in soft agar. However, the size of the colonies was doubled (Figure 5D). CXCL12 expressing TOSE cells still failed to grow in SCID mice when implanted s.c. or i.p.

CXCR4, p53 and EGFR pathway expression in serous ovarian cancer biopsies

TOSE cells demonstrate altered CXCR4 and p53 expression. To investigate whether CXCR4 and p53 are linked in patient biopsies, we tested whether a recently defined mutated *TP53* gene expression signature (28) was associated with increased expression of CXCR4 pathway genes. This mutated *TP53* gene expression signature was observed in 50 samples selected for highest levels of CXCR4 pathway gene expression ($p=0.0089$): high CXCR4 pathway expression is indicative of mutated *TP53* expression profiles. Samples selected for high CXCR4 pathway expression was also associated with down-regulation of p53 target genes ($p<0.001$) (Figure 6A). In HGSOC, we conclude that mutated *TP53* expression signature and decreased expression of p53 target genes are associated with high expression of CXCR4 pathway genes.

As TOSE shCXCR4 cells resulted in reduced EGFR expression (Figure 4A, B), we also tested whether EGFR pathway genes were enriched in patient samples selected for high CXCR4 pathway expression. Genes differentially regulated between high CXCR4 and low CXCR4 pathways are enriched with genes from the EGFR pathway ($p=<0.001$) (Figure 6B).

Discussion

Controversy remains over the cell of origin of HGSOC and the precise molecular events that occur during cellular transformation. Our data indicate that cultures taken from the ovarian surface epithelium can transform into cells with mutations in *TP53* and other genomic changes that are typical of advanced stages HGSOC. However, we cannot exclude the possibility that the NOSE25 cells collected from brushings from the ovarian surface epithelium may be fallopian in origin, given the close proximity of these two tissues and the common finding of endosalpingiosis in the female pelvis.

The TOSE cells were not fully malignant. However, they fulfilled the other markers of transformation: growth in soft agar, cytogenetic changes and alterations in morphology. TOSE cells also showed increased sensitivity to the oncolytic adenovirus *dl*922-947 when compared with parental IOSE cells, suggesting that they have altered Rb pathways (29).

Following long-term culture, normal murine OSE and rat OSE cells transform spontaneously (30-32). However, human cells need to overcome greater barriers than murine

cells to reach malignancy (33). Soft agar may provide one selection pressure. In addition, the parental IOSE25 cells, although obtained from a donor without malignant ovarian disease, contained a missense heterozygous mutation in exon 5 of *TP53*, which may have contributed to cellular transformation, as this mutation is implicated in the development of chromosomal aberrations through inhibition of DNA ligation (34). TOSE cells lost the mutant allele and gained a different *TP53* missense mutation in exon 8 of the remaining allele, in a location that is commonly mutated in ovarian cancer (6). Loss of the wild-type allele of *TP53* has not been carefully reported in HGSOC (6, 35) although our unpublished data estimate this in at least 80% of cases. In targeted human cell lines and in mouse models, loss of the wild-type allele confers significant advantage for the transformed cell (35, 36). Loss of the wild-type allele may also be critical in human cancers as gain-of-function mutations in *TP53* may be more important than putative dominant-negative effects (37) (38). We can only speculate as to how a second mutation arose in the TOSE lines as synchronous mutations in *TP53* are not reported, although different mutations have been observed between p53 signature lesions in the normal fallopian tube and HGSOC tissues (39).

As NOSE25 cells (from which the immortal cells were derived) had a very small population with R175H mutation, it is possible that, together with hTERT, these cells had a survival advantage *in vitro*. We cannot exclude the possibility that there was an even smaller population of cells with the R273H mutation that were not detected, even by digital PCR. It is important to note that HGSOC shows distinct cellular heterogeneity (40). Preferential selection of TOSE mutant R273H clone may have occurred because R273H has greater dominant-negative function and tumor promoting properties than the R175H allele (35). In addition, the resultant hemizygous minor Arg72 allele has increased allelic expression of p53 when compared with Pro72 allele (41). These observations are supported by data in this paper showing that TOSE cells have greater p53 immunoreactivity than IOSE25 cells. TOSE cells also demonstrated a change in expression of *TP53* target genes compared with IOSE25, suggesting that the *TP53* mutation in exon 8, *TP53* LOH and nuclear immunoreactivity are associated with functional changes of p53 in TOSE cells.

TOSE cells contained a genomic amplification of the chemokine receptor CXCR4. This, to our knowledge, is the first report of chemokine receptor amplification. Chemokines and their receptors have important roles in cancer especially during metastasis (42). Our results indicate that at least one chemokine receptor could be important in the early stages of cell transformation and suggest that CXCR4 and p53 pathways are linked in human ovarian cancers.

Gene amplicons are found in pre-neoplastic tissue (43), and amplicons are indicative of candidate oncogenes (44). Santarius *et al* proposed criteria for identifying oncogenes in areas that are amplified in cancer (45). In ovarian cancer, *CXCR4* fulfils these criteria: CXCR4 expression correlates with clinical evidence (14); CXCR4 expression leads to alterations in other genes in the same pathway; alterations in expression causes a biological effect and there is substantial evidence from animal studies (15, 24, 25). However, as yet we have no evidence of *CXCR4* amplification in HGSOC biopsies. Furthermore, amplification of *CXCR4* may occur in precursor cells, but lost upon full malignancy.

Our data suggest that CXCR4 expression and *TP53* mutation are intrinsically linked in ovarian cancer. In breast cancer, wild type but not mutant *TP53* represses CXCR4 expression and p53 rescue drugs (PRIMA-1 and CP-31398) reduced CXCR4 expression (46). It was also recently suggested that *TP53* mutation in cancer stem cells leads to CXCR4 up-regulation (47).

TOSE cells have epigenetically silenced CXCL12. Cells with epigenetically silenced CXCL12 have increased metastatic potential in mammary carcinoma (27), as they are able to follow chemokine gradients. There is increasing evidence for a new model of metastasis: pre-malignant cells migrate to distant sites of metastasis where they accumulate more mutations independently before growing tumors (48). TOSE cells may represent pre-malignant HGSOC lesions that through epigenetically silenced CXCL12 are able to disseminate. They do not have sufficient genetic changes to form cancers, but further selection pressures may eventually lead to tumor growth.

CXCL12 expression is increased in late stage ovarian cancers and contributes to tumor growth (22). In order for full malignancy to progress, any epigenetic silencing would need to be overcome. However, TOSE-CXCL12 cells did not grow when implanted into SCID mice, indicating that further abnormalities are necessary for full malignancy.

TOSE cells also display an enriched EGFR pathway, suggesting that these ‘precursor’ cells are primed to potentially interact with their ligands and have a survival advantage. It is proposed that cross-talk exists between CXCL12/CXCR4 and EGFR intracellular pathways that link signals of cell proliferation in ovarian cancer (49). Understanding the significance of CXCR4 signalling in the earliest stages of HGSOC will require further study.

Materials and methods

Ovarian cell lines

Ovarian surface epithelial cells (IOSE25) immortalised and cultured as described (12). IGROV-1 cells obtained from Dr Martin Ford (Glaxo R&D Stevenage, UK) in 1998 and last underwent 16 loci STR authentication (LGC Standards, London, UK) in September 2011. They were cultured in RPMI 1640 supplemented with 10% FCS.

Cells were treated with 100ng/ml CXCL12 (Peprotech, Rocky Hill, NJ), 1μg/ml AMD3100 (Sigma, St Louis, MA) or 100μg/ml CTCE-9908 (Chemokine Therapeutic Corp., Vancouver, Canada). Cell counts/circularity performed using Vi-Cell™ cell viability analyser (Beckman Coulter, High Wycombe, UK).

Microsatellite analysis

Fluorescently labelled primers (Applied Biosystems, CA, USA) amplified eight loci (Applied Biosystems Linkage mapping set) covering four chromosomes. Cycling parameters on MJ tetrad PCR blocks: 95°C ×10 min, 35 cycles of 95°C × 30 sec, 60°C × 30 sec, 72°C × 30 sec. PCR product combined with ROX400HD size standard (Applied Biosystems) and HiDi Formamide (Applied Biosystems), heat denatured at 95°C for 5 minutes, visualised using 3730 capillary sequencing instrument (Applied Biosystems) and genotypes called using GeneMapper (Applied Biosystems).

TP53 sequencing and digital PCR

Sequencing of exons 2–11 and intron-exon boundaries of *TP53* performed as described (50) with following modifications: PCR reactions performed in 25μl; universal M13 forward and M13 reverse sequences included for bidirectional sequencing of each exon an alternative forward primer sequence of CAGGTCTCCCCAAGGCGCAC for sequencing exon 7 to avoid poor quality sequence from a poly A tract adjacent to previously described primer. Sequence data from *TP53* aligned to reference NC_000017.0. Sequencing of *KRAS*, *BRAF*, *CTNNB1* and *PIK3CA* and mutational analysis performed as described (6). Digital PCR was performed using the Fluidigm Biomark microfluidic system according to manufacturer’s instructions. Samples were heated to 95°C for 1 minute and placed on ice.

Reaction mixes contained 1ul of 4ng/ul cell line DNA, TaqMan Universal PCR mastermix (Applied Biosystems), 1 × GE loading buffer (Fluidigm), 1800nM forward and reverse primers and 400nM of each germline and tumor-specific probe. Samples loaded onto a 12.765 Fluidigm digital chip containing 12 panels with each containing 765 chambers with a 6nl reaction volume and thermocycled at 50°C for 2 minutes; 95°C for 10 minutes followed by 55 cycles of 95°C for 15s and 60°C for 1 minute.

***TP53*R175H**	
CXP015B_F	CCATCTACAAGCAGTCAC
CXP015B_R	TCACCATCGCTATCTGAG
CXP015B_T_FAM	[6FAM]TTGTGAGGCACTGCCCCC[BHQ1]
CXP015B_N_HEX	[HEX]TTGTGAGGCGCTGCCCCC[BHQ1]
***TP53*R273H**	
CXP024B_F	GGACCTGATTTCCTTACTG
CXP024B_R	GGAGATTCTCTTCCTCTGTG
CXP024B_T_FAM	[6FAM]AGGCACAAACATGCACCTCAAAG[BHQ1]
CXP024B_N_HEX	[HEX]AGGCACAAACACGCACCTCAAAG[BHQ1]

Soft agar assay

5×10^4 cells added to 0.35% agar in MCDB105/M199 supplemented medium above a base layer of 0.5% agar in 6 well plates. Following incubation, colonies stained with 0.005% crystal violet (Sigma) and scored.

Expression arrays and bioinformatics analysis

RNA isolated using standard Trizol protocol, purified further with RNeasy kit (Qiagen) according to manufacturer's recommendations. Affymetrix GeneChip Human Genome U133 Plus 2.0 arrays used. Probe synthesis and microarray hybridization performed according to standard Affymetrix (Santa Clara, CA) protocols at Barts Cancer Institute. Triplicate samples obtained per cell line. Microarray samples deposited at NCBI's Gene Expression Omnibus repository (GSE13763). Data analyzed using Bioconductor 2.5 [http://bioconductor.org] running on R version 2.10.0 (51). Probeset expression measures calculated using Affymetrix Robust Multichip Average (RMA) default method (52). Differential gene expression assessed between IOSE and TOSE sample groups using an empirical Bayes t-test (limma package) (53). P values adjusted for multiple testing correction using Benjamini-Hochberg method (54). 2D hierarchical clustering of expression data using differentially expressed genes (adjusted p value of 0.05 or more) between IOSE and TOSE samples performed. Samples clustered using 1 - Pearson correlation distance matrix and average linkage clustering. Genes clustered using Euclidean distance matrix and average linkage clustering using Cluster and visualized using Java TreeView (55)

p53 target genes and CXCR4 pathway genes extracted from Metacore pathway tool (GeneGo Inc, St. Joseph, MI). These are listed in Supplementary tables S2 and S6.

Copy number and loss of heterozygosity analysis

Genomic DNA from cell lines extracted using DNA mini kit (Qiagen, Hilden, Germany) and analysed using Genome-Wide Human SNP Array 6.0 (Affymetrix) according to manufacturer's instructions.

Data deposited at NCBI's repository (GSE25492). In-house Genome Orientated Laboratory File (GOLF) package used for data analysis. Hybridisation values normalised to median value on each array, and copy number determined based on $\log_2$ ratio of signal intensity of TOSE DNA compared with IOSE25 DNA.

FISH

Human BAC clone for CXCR4 (clone 809c23 from RPCI11.C) labelled with SpectrumGreen dUTP (Abbot Molecular, Illinois, US) using nick translation enzyme (Abbot Molecular). Colcemid (2ng/ml; Sigma) treatment overnight arrested cells in metaphase, and cells fixed with 3:1 methanol: acetic acid, dropped on slides, aged at 60°C for 20 min, rinsed (2X SSC, 30 min, 37°C) and dehydrated in an ethanol series. CXCR4 amplification was assessed using labelled BAC clone and a control probe for chromosome 2 centromere (CEP2) labelled with SpectrumOrange (Abbott Molecular). HyBrite denaturation/ hybridisation system used (probes and slides co-denatured at 73°C, 5 min). Hybridisation was carried out for 18hr at 37°C, followed by washes in 0.4X SSC plus Tween (0.4%). Slides were counterstained with DAPI Prolong Gold (Molecular Probes, Invitrogen) and images captured by Nikon Eclipse 80i microscope and Image-Pro Plus software (Media Cybernetics).

RNA extraction and real-time quantitative reverse transcription PCR analysis

RNA was extracted from cell lines using Qiagen RNeasy (Qiagen). DNase treated RNA reverse transcribed with Moloney murine leukaemia virus reverse transcriptase (Promega, Southampton, UK) and real-time reverse transcription PCR analysis carried out using EGFR, CXCR4 or CXCL12 (FAM) and 18s rRNA (VIC) specific primers and probes with ABI PRISM 7700 Sequence Detection System instrument and software (PE Applied Biosystem, Warrington, UK). Expression values were normalised (ΔCt) to 18s rRNA. Fold difference = $2^{-(\Delta Ct)}$

Western Blotting

Cell lysates run on 10% NuPAGE gels (Invitrogen), transferred to PVDF membrane (Millipore). Antibodies against CXCR4 (Abcam, Cambridge, UK), EGFR (Cell Signaling, Boston, MA) and β–actin (Sigma) followed by a horseradish peroxidase-conjugated secondary antibody (GE Healthcare, Chalfont St Giles, UK) incubation allowed visualisation using enhanced chemiluminescence (ECL) (GE Healthcare).

Immunofluoresence staining

Cells plated on Lab-Tek chamber slides (Nalge Nunc International, ThermoFisher Scientific, Rochester, NY, US), fixed with paraformaldehyde (4%) and permeabilised in 0.5% Triton X-100, washed in 0.1% Triton X-100 and stained overnight with p53 (BD Biosystems) or isotype control (R&D systems) antibodies (1:200). Primary antibodies were washed with PBS and Alexa Fluor 488 secondary antibody (Invitrogen) applied. Slides were counterstained with DAPI Prolong Gold (Invitrogen) and images captured by Nikon Eclipse 80i microscope and Image-Pro Plus software (Media Cybernetics).

Cell motility assay

Cell migration was assayed using Falcon Transwells (24-well format, 8μm pore; BD Biosciences). 5×10^5 IOSE or TOSE cells (pretreated with AMD3100 (1μg/ml), CTCE9908 (100μg/ml) or control for 15 min) were added to upper chamber, and medium alone or medium supplemented with CXCL12 was added to lower chamber. Following incubation for 18 h at 37°C in 5% CO_2, migrated cells to lower chamber were stained using DiffQuick (Dade Behring, Düdingen, Switzerland) and counted.

CXCR4 shRNA transfection

TOSE cells were transfected with pSilencer containing a hairpin sequence against CXCR4 (Ambion, Austin, TX, US) using siPORT XP-1 (Ambion). Selection with hygromycin (100μg/ml) was carried out after 24 hours for 30 days.

CXCL12 ELISA

CXCL12 concentrations in cell supernatants (72h culture) measured using Quantikine ELISA kits following manufacturer's instructions (R&D Systems). Sensitivity of assay: 18pg/ml.

Bisulfite treatment and methylation specific PCR

Genomic DNA (2μg) was bisulfite treated using EpiTect Bisulfite kit (Qiagen). Methylation specific PCR was carried out as previously described (26).

Demethylation

TOSE cells treated with 5-aza-2′-deoxycytidine (2μM) for 5 days, and/or trichostatin A (100ng/ml) for 24 hours before RNA extraction, cDNA generation and RT PCR analysis as described previously.

Statistical analysis

Statistical analysis carried out using Prism Graph Pad software. Statistical significance was calculated using Student's t test.

Supplementary Material

Refer to Web version on PubMed Central for supplementary material.

Acknowledgments

We thank Nitzan Rosenfeld and Davina Gale for their expert advice and analysis for the *TP53* quantification. We also thank Debra Lillington for karyotyping TOSE cells, and the Genome Centre at Barts and the London School of Medicine and Dentistry for microsatellite analysis.

This work was supported by Cancer Research UK, the Association for International Cancer Research and HEFCE.

References

1. Vaughan S, Coward J, Bast RC Jr, Berchuck A, Berek JS, Brenton JD, et al. Rethinking ovarian cancer: recommendations for improving outcomes. Nature Reviews Cancer. 2011; 11:719–725.
2. Farley J, Ozbun LL, Birrer MJ. Genomic analysis of epithelial ovarian cancer. Cell Res. May; 2008 18(5):538–48. [PubMed: 18427574]
3. Piek JM, van Diest PJ, Zweemer RP, Jansen JW, Poort-Keesom RJ, Menko FH, et al. Dysplastic changes in prophylactically removed Fallopian tubes of women predisposed to developing ovarian cancer. J Pathol. Nov; 2001 195(4):451–6. [PubMed: 11745677]
4. Lee Y, Miron A, Drapkin R, Nucci MR, Medeiros F, Saleemuddin A, et al. A candidate precursor to serous carcinoma that originates in the distal fallopian tube. J Pathol. Jan; 2007 211(1):26–35. [PubMed: 17117391]
5. Levanon K, Ng V, Piao HY, Zhang Y, Chang MC, Roh MH, et al. Primary ex vivo cultures of human fallopian tube epithelium as a model for serous ovarian carcinogenesis. Oncogene. Feb 25; 2010 29(8):1103–13. [PubMed: 19935705]
6. Ahmed AA, Etemadmoghadam D, Temple J, Lynch AG, Riad M, Sharma R, et al. Driver mutations in TP53 are ubiquitous in high grade serous carcinoma of the ovary. J Pathol. May; 2010 221(1):49–56. [PubMed: 20229506]

7. Network TCGAR. Integrated genomic analyses of ovarian carcinoma. Nature. Jun 30.2011 474:609–15. 2011. [PubMed: 21720365]
8. Press JZ, De Luca A, Boyd N, Young S, Troussard A, Ridge Y, et al. Ovarian carcinomas with genetic and epigenetic BRCA1 loss have distinct molecular abnormalities. BMC Cancer. 2008; 8:17. [Research Support, N.I.H., Extramural Research Support, Non-U.S. Gov't Research Support, U.S. Gov't, Non-P.H.S.]. [PubMed: 18208621]
9. Jazaeri AA, Bryant JL, Park H, Li H, Dahiya N, Stoler MH, et al. Molecular requirements for transformation of fallopian tube epithelial cells into serous carcinoma. Neoplasia. Oct; 2011 13(10): 899–911. [PubMed: 22028616]
10. Karst AM, Levanon K, Drapkin R. Modeling high-grade serous ovarian carcinogenesis from the fallopian tube. Proceedings of the National Academy of Sciences of the United States of America. May 3; 2011 108(18):7547–52. [Research Support, N.I.H., Extramural Research Support, Non-U.S. Gov't]. [PubMed: 21502498]
11. Mehra K, Mehrad M, Ning G, Drapkin R, McKeon FD, Xian W, et al. STICS, SCOUTs and p53 signatures; a new language for pelvic serous carcinogenesis. Front Biosci (Elite Ed). 2011; 3:625–34. [Research Support, N.I.H., Extramural Research Support, Non-U.S. Gov't Review]. [PubMed: 21196340]
12. Li NF, Broad S, Lu YJ, Yang JS, Watson R, Hagemann T, et al. Human ovarian surface epithelial cells immortalised with hTERT maintain function prb and p53 expression. Cell Proliferation. 2007; 40:780–94. [PubMed: 17877616]
13. Scotton CJ, Wilson JL, Milliken D, Stamp G, Balkwill FR. Epithelial cancer cell migration: a role for chemokine receptors? Cancer Res. 2001; 61:4961–5. [PubMed: 11431324]
14. Kajiyama H, Shibata K, Terauchi M, Ino K, Nawa A, Kikkawa F. Involvement of SDF-1a/CXCR4 axis in the enhanced peritoneal metastasis of epithelial ovarian carcinoma. Int J Cancer. 2008; 122:91–9. [PubMed: 17893878]
15. Kulbe H, Chakravarty P, Leinster DA, Charles KA, Kwong J, Thompson RG, et al. A dynamic inflammatory cytokine network in the human ovarian cancer microenvironment. Cancer research. Nov 7.2011
16. Singer G, Stohr R, Cope L, Dehari R, Hartmann A, Cao DF, et al. Patterns of p53 mutations separate ovarian serous borderline tumors and low- and high-grade carcinomas and provide support for a new model of ovarian carcinogenesis: a mutational analysis with immunohistochemical correlation. Am J Surg Pathol. Feb; 2005 29(2):218–24. [PubMed: 15644779]
17. Micci F, Haugom L, Ahlquist T, Abeler VM, Trope CG, Lothe RA, et al. Tumor spreading to the contralateral ovary in bilateral ovarian carcinoma is a late event in clonal evolution. J Oncol. 2010; 2010:646340. [PubMed: 19759843]
18. Kuo KT, Guan B, Feng Y, Mao TL, Chen X, Jinawath N, et al. Analysis of DNA copy number alterations in ovarian serous tumors identifies new molecular genetic changes in low-grade and high-grade carcinomas. Cancer Res. May 1; 2009 69(9):4036–42. [PubMed: 19383911]
19. Nakayama K, Nakayama N, Jinawath N, Salani R, Kurman RJ, Shih Ie M, et al. Amplicon profiles in ovarian serous carcinomas. Int J Cancer. Jun 15; 2007 120(12):2613–7. [PubMed: 17351921]
20. Dimova I, Orsetti B, Negre V, Rouge C, Ursule L, Lasorsa L, et al. Genomic markers for ovarian cancer at chromosomes 1, 8 and 17 revealed by array CGH analysis. Tumori. May-Jun;2009 95(3): 357–66. [PubMed: 19688977]
21. Etemadmoghadam D, deFazio A, Beroukhim R, Mermel C, George J, Getz G, et al. Integrated genome-wide DNA copy number and expression analysis identifies distinct mechanisms of primary chemoresistance in ovarian carcinomas. Clin Cancer Res. 2009; 15:1417–27. [PubMed: 19193619]
22. Scotton CJ, Wilson JL, Scott K, Stamp G, Wilbanks GD, Fricker S, et al. Multiple actions of the chemokine CXCL12 on epithelial tumor cells in human ovarian cancer. Cancer Research. 2002; 62:5930–8. [PubMed: 12384559]
23. Balabanian K. The chemokine SDF-1/CXCL12 binds to and signals through the orphan receptor RDC1 in T lymphocytes. J Biol Chem. 2005; 280:35760–6. al e. [PubMed: 16107333]

24. Kulbe H, Hagermann T, Szlosarek PW, Balkwill FR, Wilson JL. The inflammatory cytokine TNF-a upregulates chemokine receptor expression on ovarian cancer cells. Cancer Res. 2005; 65:10355–62. [PubMed: 16288025]
25. Kulbe H, Thompson RT, Wilson J, Robinson SC, Hagemann T, Fatah R, et al. The inflammatory cytokine TNF-a generates an autocrine tumour-promoting network in epithelial ovarian cancer cells. Cancer Res. 2007; 67:585–92. [PubMed: 17234767]
26. Wendt MK, Johanesen PA, Kang-Decker J, Binion DG, Shah V, Dwinell MB. Silencing of epithelial CXCL12 expression by DNA hypermethylation promotes colonic carcinoma metastasis. Oncogene. 2006; 25:4986–97. [PubMed: 16568088]
27. Wendt MK, Cooper AN, Dwinell MB. Epigenetic silencing of CXCL12 increases the metastatic potential of mammary carcinoma cells. Oncogene. Feb 28; 2008 27(10):1461–71. [PubMed: 17724466]
28. Bernardini MQ, Baba T, Lee PS, Barnett JC, Sfakianos GP, Secord AA, et al. Expression signatures of TP53 mutations in serous ovarian cancers. BMC Cancer. 2010; 10:237. [PubMed: 20504346]
29. Flak MB, Connell CM, Chelala C, Archibald K, Salako MA, Pirlo KJ, et al. p21 Promotes oncolytic adenoviral activity in ovarian cancer and is a potential biomarker. Mol Cancer. 2010; 9:175. [PubMed: 20598155]
30. Godwin AK, Testa JR, Handel LM, Liu Z, Vanderveer LA, Tracey PA, et al. Spontaneous transformation of rat ovarian surface epithelial cells: association with cytogenetic changes and implications of repeated ovulation in the etiology of ovarian cancer. JNCI. 1992; 84:592–601. [PubMed: 1556770]
31. Roby KF, Taylor CC, Sweetwood JP, Cheng Y, Pace JL, Tawfik O, et al. Development of a syngeneic mouse model for events related to ovarian cancer. Carcinogenesis. 2000; 21:585–91. [PubMed: 10753190]
32. Testa JR, Getts LA, Salazar H, Liu Z, Handel LM, Godwin AK, et al. Spontaneous transformation of rat ovarian surface epithelial cells results in well to poorly differentiated tumors with a parallel range of cytogenetic complexity. Cancer Res. 1994; 54:2778–84. [PubMed: 8168110]
33. Hahn WC, Weinberg RA. Modelling the molecular circuitry of cancer. Nature Reviews. 2002; 2:331–41.
34. Okorokov AL, Warnock L, Milner J. Effect of wild-type, S15D and R175H p53 proteins on DNA end joining in vitro: potential mechanism of DNA double-strand break repair modulation. Carcinogenesis. Apr; 2002 23(4):549–57. [PubMed: 11960905]
35. Jackson EL, Olive KP, Tuveson DA, Bronson R, Crowley D, Brown M, et al. The differential effects of mutant p53 alleles on advanced murine lung cancer. Cancer research. Nov 15; 2005 65(22):10280–8. [Research Support, N.I.H., Extramural Research Support, Non-U.S. Gov't]. [PubMed: 16288016]
36. Sur S, Pagliarini R, Bunz F, Rago C, Diaz LA Jr. Kinzler KW, et al. A panel of isogenic human cancer cells suggests a therapeutic approach for cancers with inactivated p53. Proceedings of the National Academy of Sciences of the United States of America. Mar 10; 2009 106(10):3964–9. [Research Support, N.I.H., Extramural Research Support, Non-U.S. Gov't]. [PubMed: 19225112]
37. Olive KP, Tuveson DA, Ruhe ZC, Yin B, Willis NA, Bronson RT, et al. Mutant p53 gain of function in two mouse models of Li-Fraumeni syndrome. Cell. Dec 17; 2004 119(6):847–60. [Research Support, Non-U.S. Gov't Research Support, U.S. Gov't, P.H.S.]. [PubMed: 15607980]
38. Stoczynska-Fidelus E, Szybka M, Piaskowski S, Bienkowski M, Hulas-Bigoszewska K, Banaszczyk M, et al. Limited importance of the dominant-negative effect of TP53 missense mutations. BMC cancer. 2011; 11:243. [Research Support, Non-U.S. Gov't]. [PubMed: 21668955]
39. Kindelberger DW, Lee Y, Miron A, Hirsch MS, Feltmate C, Medeiros F, et al. Intraepithelial carcinoma of the fimbria and pelvic serous carcinoma: Evidence for a causal relationship. The American journal of surgical pathology. Feb; 2007 31(2):161–9. [Research Support, N.I.H., Extramural Research Support, Non-U.S. Gov't]. [PubMed: 17255760]
40. Cooke SL, Ng CK, Melnyk N, Garcia MJ, Hardcastle T, Temple J, et al. Genomic analysis of genetic heterogeneity and evolution in high-grade serous ovarian carcinoma. Oncogene. Sep 2; 2010 29(35):4905–13. [Research Support, Non-U.S. Gov't]. [PubMed: 20581869]

41. Maia AT, Spiteri I, Lee AJ, O'Reilly M, Jones L, Caldas C, et al. Extent of differential allelic expression of candidate breast cancer genes is similar in blood and breast. Breast Cancer Res. 2009; 11(6):R88. [Research Support, Non-U.S. Gov't]. [PubMed: 20003265]
42. Zlotnik A. Chemokines and cancer. Int J Cancer. 2006; 119:2026–9. [PubMed: 16671092]
43. Roh HJ, Shin DM, Lee JS, Ro JY, Tainsky MA, Hong WK, et al. Visualization of the timing of gene amplification during multistep head and neck tumorigenesis. Cancer Res. Nov 15; 2000 60(22):6496–502. [PubMed: 11103819]
44. Albertson DG. Gene amplification in cancer. Trends Genet. 2006; 22:447–55. [PubMed: 16787682]
45. Santarius T, Shipley J, Brewer D, Stratton MR, Cooper CS. A census of amplified and overexpressed human cancer genes. Nat Rev Cancer. Jan; 10(1):59–64. [PubMed: 20029424]
46. Mehta SA, Christopherson KW, Bhat-Nakshatri P, Goulet RJ Jr. Broxmeyer HE, Kopelovich L, et al. Negative regulation of chemokine receptor CXCR4 by tumor suppressor p53 in breast cancer cells: implications of p53 mutation or isoform expression on breast cancer cell invasion. Oncogene. May 17; 2007 26(23):3329–37. [PubMed: 17130833]
47. Katoh M. Integrative genomic analyses of CXCR4: transcriptional regulation of CXCR4 based on TGFbeta, Nodal, Activin signaling and POU5F1, FOXA2, FOXC2, FOXH1, SOX17, and GFI1 transcription factors. Int J Oncol. Feb; 2010 36(2):415–20. [PubMed: 20043076]
48. Ansieau S, Hinkal G, Thomas C, Bastid J, Puisieux A. Early origin of cancer metastases: dissemination and evolution of premalignant cells. Cell Cycle. Dec; 2008 7(23):3659–63. [PubMed: 19029812]
49. Porcile C, Bajetto A, Barbieri F, Barbero S, Bonavia R, Biglieri M, et al. Stromal cell-derived factor-1alpha (SDF-1alpha/CXCL12) stimulates ovarian cancer cell growth through the EGF receptor transactivation. Exp Cell Res. Aug 15; 2005 308(2):241–53. [Research Support, Non-U.S. Gov't]. [PubMed: 15921680]
50. Sjoblom T, Jones S, Wood LD, Parsons DW, Lin J, Barber TD, et al. The consensus coding sequences of human breast and colorectal cancers. Science. Oct 13; 2006 314(5797):268–74. [PubMed: 16959974]
51. Team RDC. R: A Language and environment for statistical computing. R Foundation for Statistical Computing; 2008.
52. Gautier L, Cope L, Bolstad BM, Irizarry RA. Affy-analysis of Affymetrix GeneChip data at the probe level. Bioinformatics. 2004; 20:307–15. [PubMed: 14960456]
53. Smyth GK. Limma: linear models for microarray data. Bioinformatics and Computational Biology Solutions using R and Bioconductor. 2005:397–420.
54. Benjamini Y, Hochberg Y. Controlling the FAlse Discovery Rate: A Practical and Powerful Approach to Multiple Testing. J. Roy Stat. Soc, Ser B.
55. Saldanha AJ. Java Treeview--extensible visualization of microarray data. Bioinformatics. Nov 22; 2004 20(17):3246–8. [PubMed: 15180930]

Europe PMC Funders Author Manuscripts

Europe PMC Funders Author Manuscripts

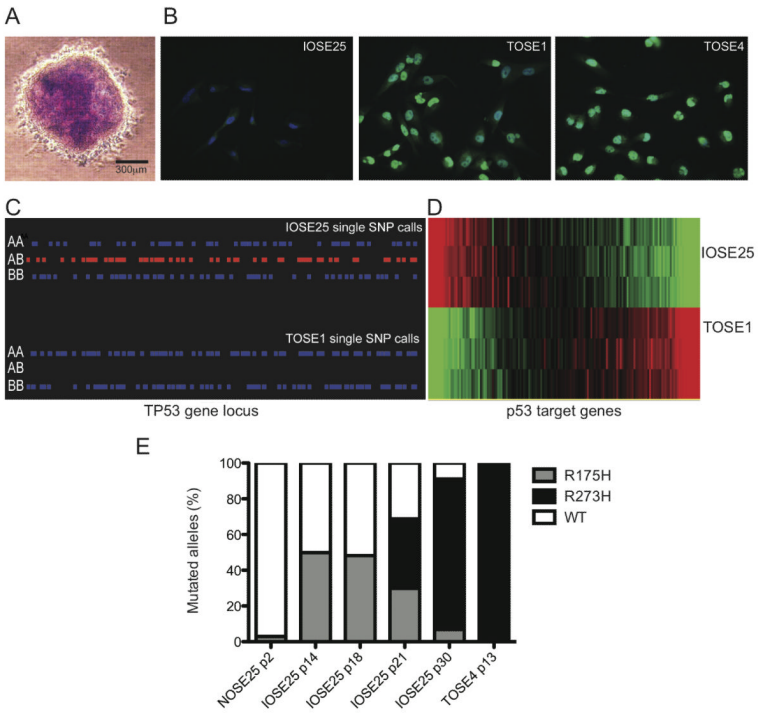

Figure 1. hTERT immortalised ovarian surface epithelial (IOSE) cells spontaneously transformed *in vitro*

(A) Photomicrograph of clonal growth in soft agar (x400). (B) Cells stained for p53 (green) and counterstained with DAPI (x400). (C) IOSE25 cells are heterozygous at *TP53* gene locus. TOSE have loss of heterozygosity at this locus. Blue: homozygous AA/BB; red: heterozygous calls. Image: chromosome 17:6,912,192-8,130,177. (*TP53* gene: 17:7,512,445-7,531,642). (D) Hierarchal clustering showing the expression profiles of p53 target genes (extracted from Metacore; three samples per group). Only probesets that showed statistical significance (FDR < 0.05) used. Red: higher expression, green: lower expression relative to the mean expression of the gene across all samples. (E) Digital PCR specific for R175H and R273H mutations for varying passages of IOSE25 cells, normal (N) OSE cells, and TOSE1 cells.

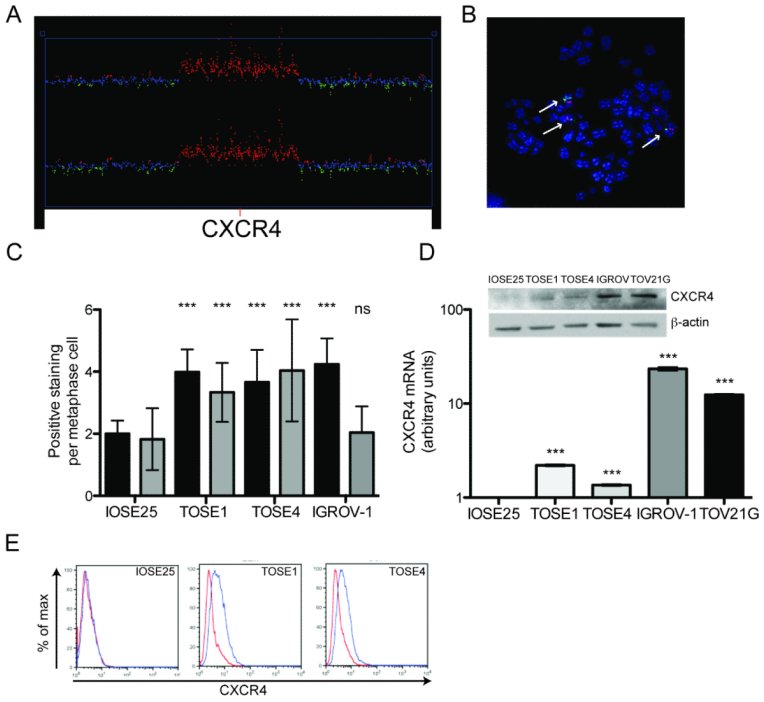

Figure 2. TOSE cells have amplified genomic CXCR4 and accompanied by increased CXCR4 mRNA and protein

(A) Copy number changes in TOSE cells analysed using high resolution SNP arrays (SNP6.0) and compared with the parental IOSE25 cells log-wise. Red: statistically significant increases in SNP signals. Discrete amplification of *CXCR4* gene shown. Image: 2:136,022,071-137,713,650. Amplicon: 2:136,588,303-137,111,749. CXCR4: 2:136,871,919. (B) Metaphase spread of TOSE1 with fluorescent *in situ* hybridisation (FISH) for CXCR4 (green) and chromosome 2 centromere (red). (C) Images scored (100 per cell line; black: chromosome 2 centromere, grey: CXCR4 probe). (D) CXCR4 mRNA expression (qRT-PCR), n=4. Student's t test compared expression with IOSE25 cells (inset: total CXCR4 protein). CXCR4 expressing cell lines IGROV-1 and TOV21G included. Molecular weight of CXCR4: 45kDa. ± SD, n=3. *** p<0.001, ** p<0.01, * p<0.05.

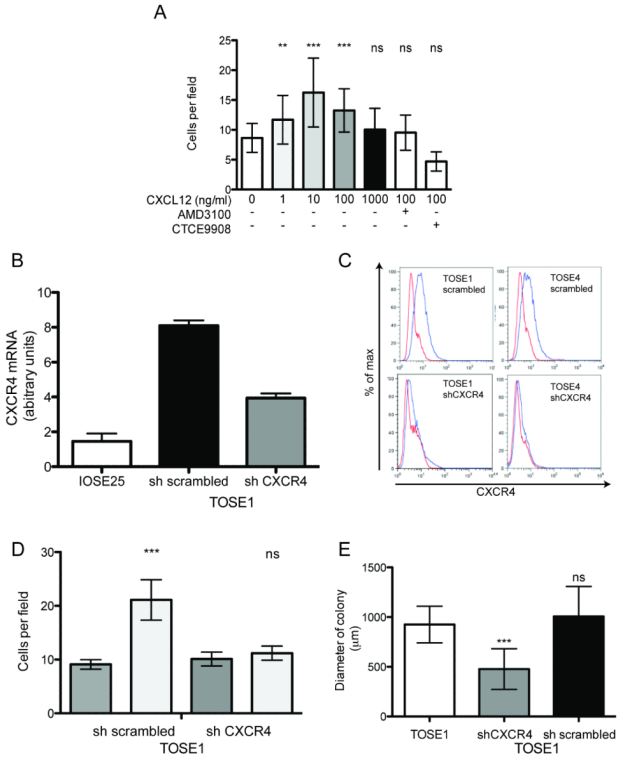

Figure 3. TOSE cells have functional CXCR4

(A) Migration of TOSE1 cells towards CXCL12 in a transwell Boyden chamber, with and without the CXCR4 inhibitors AMD3100 (1μg/ml) and CTCE9908 (100μg/ml). (B) TOSE1 cells with attenuated CXCR4 were assessed for CXCR4 expression by flow cytometry, and then migration of shCXCR4 cells with scrambled control assessed (C). TOSE1 shCXCR4 cells were grown in soft agar and size measured (D). ± SD, n=3. *** $p<0.001$, ** $p<0.01$, * $p<0.05$.

Europe PMC Funders Author Manuscripts

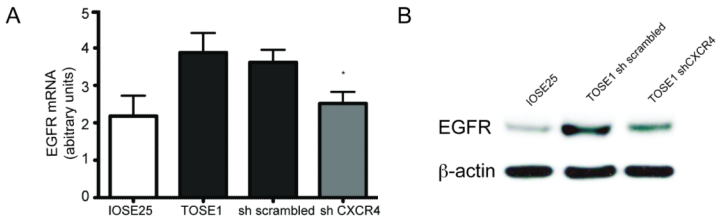

Figure 4. TOSE shCXCR4 cells have reduced EGFR expression

(A) EGFR mRNA expression (qRT-PCR), n=2. (B) EGFR protein by western blot. Blots representative of two experiments. Molecular weight of EGFR: 175kDA. ± SD, n=3. *** $p<0.001$, ** $p<0.01$, * $p<0.05$.

Europe PMC Funders Author Manuscripts

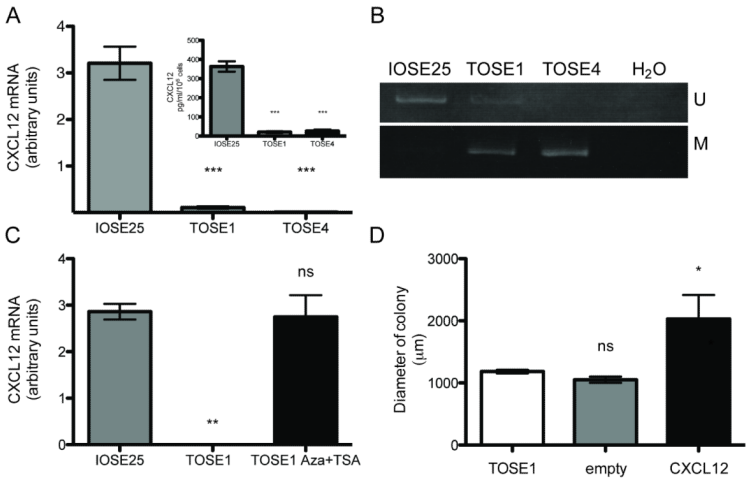

Figure 5. TOSE cells are hypermethylated at the CXCL12 promoter

(A) CXCL12 RNA levels were measured by quantitative RT-PCR. Student's t test compared TOSE cells with parental IOSE25 cells. CXCL12 protein levels measured by ELISA (inset). (B) Methylation specific PCR on bisulfite treated genomic DNA, with primers specific to unmethylated (U) or methylated (M) DNA. (C) Cells were treated with 5-aza-2′-deoxycytidine (aza) and trichostatin A (TSA) and CXCL12 RNA levels subsequently measured by quantitative RT-PCR. ± SD. Student's t test compared treated and untreated TOSE1 cells with IOSE25. CXCL12 was transduced in TOSE1 cells and size (D) of colonies in soft agar assessed. Student's t test compared modified cell lines with parental TOSE1 cells. ± SD, n=3. *** $p<0.001$, ** $p<0.01$, * $p<0.05$.

Europe PMC Funders Author Manuscripts

Europe PMC Funders Author Manuscripts

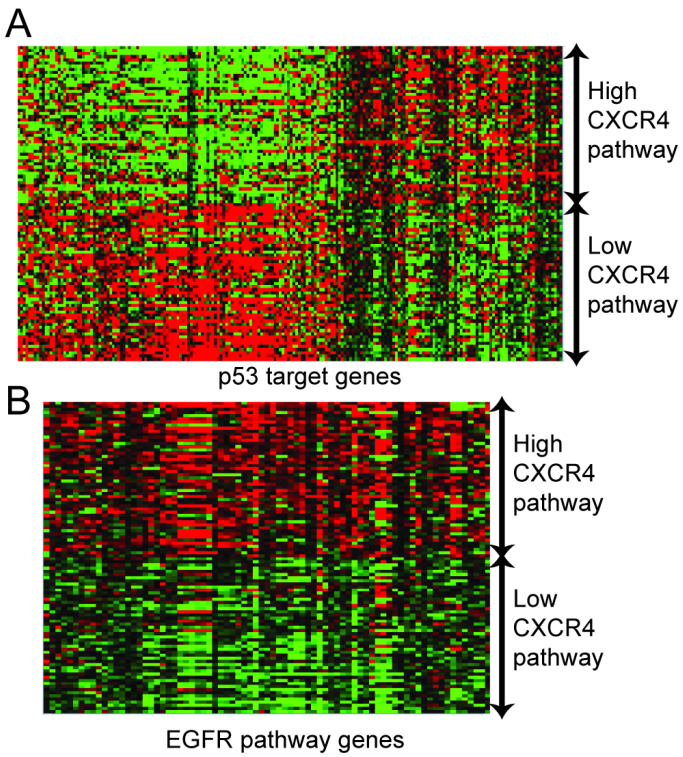

Figure 6. CXCR4 expression and p53/EGFR pathway genes in human ovarian cancer

Heatmaps of the p53 target genes (A) and EGFR pathway genes (B) against a panel of human biopsies ranked based on the expression of CXCR4 pathway genes. Samples were obtained from the publically available ovarian late (advanced) stage microarray dataset GSE9899 consisting of 285 samples. Red: higher expression, green: lower expression relative to mean expression of the gene across all samples.